UPPSALA
UNIVERSITET

Ion dynamics and structure of collisionless shocks

by

Andreas Johlander

22 Sep, 2016

DEPARTMENT OF PHYSICS AND ASTRONOMY
UPPSALA UNIVERSITY
SE-75120 UPPSALA, SWEDEN

Submitted to the Faculty of Science and Technology, Uppsala University in partial fulfillment of the requirements for the degree of Licentiate of Philosophy in Physics

Abstract

Shock waves are responsible for slowing down and heating supersonic flows. In collisionless space plasmas, shocks are able to accelerate particles to very high energies. We study injection of suprathermal ions at Earth's quasi-parallel shock using high time resolution data from the Cluster spacecraft. We find that solar wind ions reflect off short large-amplitude magnetic structures (SLAMSs) and are subsequently accelerated by the convection electric field. We also use data from the closely-spaced Magnetospheric MultiScale (MMS) spacecraft to compare competing non-stationarity processes at Earth's quasi-perpendicular bow shock. Using MMS's high cadence plasma measurements, we find that the shock exhibits non-stationarity in the form of ripples.

Vi börjar långsamt ana att den rymd vi färdas fram i är av ett annat slag än vad vi tänkt var gång ordet rymd på jorden kläddes med vår fantasi.
-Harry Martinsson, Aniara

List of papers

This thesis is based on the following papers, which are referred to in the text by their roman numerals.

I A. Johlander, A. Vaivads, Y. V. Khotyaintsev, A. Retinò, and I. Dandouras. Ion injection at Quasi-parallel Shocks Seen by the Cluster Spacecraft. Astrophys. J. Lett., 817:L4, January 2016. doi: 10.3847/2041-8205/817/1/L4

II A. Johlander, S. J. Schwartz, A. Vaivads, Yu. V. Khotyaintsev, I. Gingell, I. B. Peng, S. Markidis, et al. Rippled quasi-perpendicular shock observed by the Magnetospheric Multiscale spacecraft. Accepted to Phys. Rev. Lett.

Papers not included in this thesis

1. I. B. Peng, Markidis S., E. Laure, A. Johlander, A. Vaivads, Yu. V Khotyaintsev, P. Henri, and G. Lapenta. Kinetic structures of quasi- perpendicular shocks in global particle-in-cell simulations. Physics of Plasmas, 22(9):092109, 2015. doi: 10.1063/1.4930212.
2. Y. V. Khotyaintsev, D. B. Graham, C. Norgren, E. Eriksson, W. Li, A. Johlander, A. Vaivads, M. André, P. L. Pritchett, A. Retinò, T. D. Phan, R. E. Ergun, K. Goodrich, P.-A. Lindqvist, et al. Electron jet of asymmetric reconnection. Geophys. Res. Lett., 43:5571-5580, June 2016. doi: 10.1002/2016GL069064.

Contents

1. Introduction

Plasma is ubiquitous in the universe. The interior of stars, the interstellar medium, the solar wind and lightning on Earth is plasma. A plasma is an ionized gas consisting of charged particles, typically ions and electrons. With spacecraft orbiting around the Sun, Earth, and other planets, and even outside our solar system, we can study plasma physics in space. These studies can help us understand physical processes at other places in the universe.

Just like in neutral gases, shock waves can form in plasmas. Shocks form when an obstacle is placed in a flow with speed greater than the local sound speed. Shocks are found in many places in the universe and act to slow down and heat plasma. Shocks are also efficient particle accelerators. It is believed that shock around the remnants of supernovæare the major source of cosmic rays, extremely high energy particles that inhabit the entire galaxy.

Earth's bow shock is formed when the supersonic solar wind hits Earth's magnetic field. The bow shock shares many properties with other shocks in the universe and is a good laboratory to test models about shock physics with spacecraft observations. Shock physics is a collaborative effort of theory, simulations, laboratory experiments, and space observations.

In this thesis we study shocks using spacecraft data from the multi-spacecraft missions Cluster and Magnetospheric MultiScale. In Paper I, we study how ions are accelerated by steepened waves upstream of the shock. In Paper II, we investigate the structure of the bow shock at a certain time and find that the shock supports waves moving along the surface.

In the following chapters, we give an introduction to shock physics in space plasmas. We also give some background on Earth's bow shock and the spacecraft missions we use data from. Thereafter, we make introductions to particle acceleration and shock non-stationarity, which are the subjects of the two papers.

2. Physics of collisionless shocks

2.1 Shocks in the universe

Plasma is the the fourth state state of matter and consists of free charge carriers. Most plasmas in the universe carries a magnetic field. A plasma is considered to be *collisionless* when it is tenuous enough that the collisional mean free path is much greater than the associated scales. Collisionless plasmas are found in astrophysical plasmas such as the interstellar medium, and throughout the heliosphere in the solar wind and planetary magnetospheres. In a collisionless plasma the magnetic field plays the role collisions play in neutral gases of exchanging energy between particles and propagating waves.

Like in a neutral gas, shock waves can form in collisionless plasmas [De Hoffmann and Teller, 1950]. When an obstacle is placed in a flow with speed greater than the local sound speed of the medium, there is no way for waves to propagate upstream and ”warn” the flow of the obstacle. This results in the formation of a shock, which is a very thin transition region where the supersonic flow is slowed and heated.

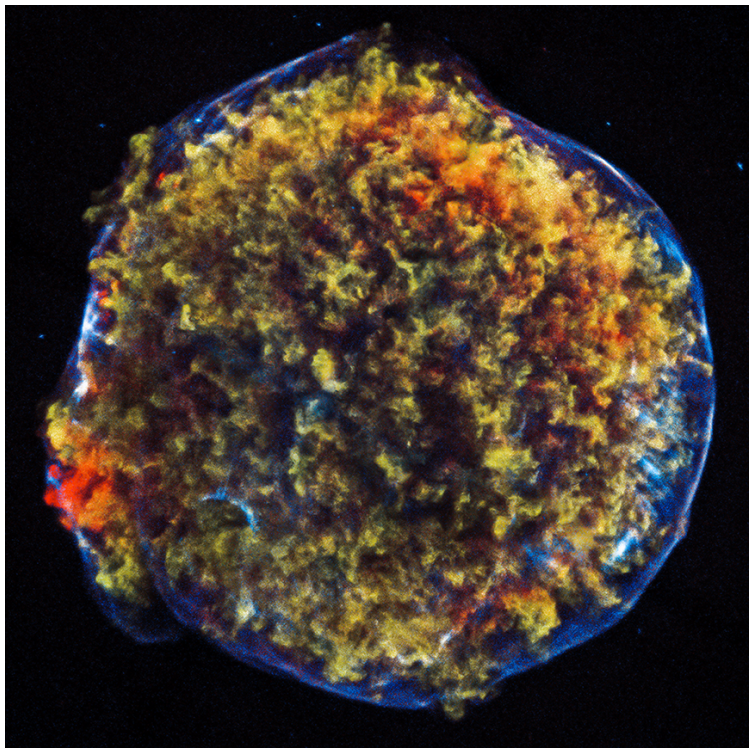

Figure 2.1. Tycho’s supernova remnant in X-rays by Chandra X-ray Observatory. Image credit: NASA/CXC/SAO.

Shocks are abundant in collisionless plasmas in the universe. In the heliosphere, they form when the supersonic solar wind hits with the magnetosphere of planets, forming planetary bow shocks. A termination shock is also formed when the solar wind is slowed before hitting the interstellar medium. When a faster portion of the solar wind overtakes a slower portion, an interplanetary shock is formed. In the solar corona, shocks are generated by solar eruptions. In astrophysical plasmas, shocks are formed for example at supernova remnants (SNRs) when the ejected material sweeps up the surrounding interstellar medium.

Collisionless shocks are efficient particle accelerators. Supernova remnant shocks are very large and energetic shocks and are most likely the source of very high energy cosmic rays. Figure 2.1 shows a supernova remnant known as Tycho's supernova in X-rays The shock is visible as a shell around the remnant. The X-rays are due to synchrotron radiation from shock accelerated electrons [Reynolds, 2008].

Collisionless shocks play an important role in slowing and thermalizing plasma, and accelerating particles to very high energies. There are still many open questions about the small scale structure, particle dynamics, acceleration mechanisms of shocks.

2.2 Shock formation

Shocks are steepened waves that act as a transition layer between the cold, and fast upstream medium and the the heated and slowed downstream medium. In a collisionless plasma, a shock forms when an obstacle in a flow that is either super-Alfvénic or super-magnetosonic. The speed of an Alfvén wave in a plasma is

$$v_A = \frac{B}{\sqrt{\mu_0 n m_i}}, \tag{2.1}$$

where B is the magnetic field magnitude and m_i is the mass of the ions in the plasma. The phase speed of a magnetosonic wave is

$$v_{ms}^2(\theta) = \frac{c_{ms}^2}{2} \pm \sqrt{\frac{c_{ms}^4}{4} - v_A^2 c_s^2 \cos^2\theta}, \tag{2.2}$$

where θ is the angle between the magnetic field and wave vector $\mathbf{k}$,

$$c_{ms}^2 = (v_A^2 + c_s^2), \tag{2.3}$$

and c_s is the ion acoustic speed

$$c_s^2 = \frac{\gamma_e k_B T_e + \gamma_i k_B T_i}{m_i}, \tag{2.4}$$

where $\gamma_{e,i}$ are specific heats for electrons and ions and $T_{e,i}$ are temperatures. The two solutions to (2.2) represent the *fast* magnetosonic wave with speed v_{ms}^{+} and the *slow* magnetosonic speed v_{ms}^{-}. A shock forms when the plasma bulk speed relative to the obstacle V is higher than one of these phase speeds $v_{ms}^{-} < v_A < v_{ms}^{+}$. Therefore, three types of shocks exist, *slow* mode, *intermediate* (Alfvénic) and *fast* mode shocks.

Among the three shock modes, the fast mode shock is the only mode that can propagate perpendicular to the magnetic field. Planetary bow shocks, the Sun's termination shock, and supernova remnant shocks are all fast mode shocks. A fast mode shock is formed when the *magnetosonic Mach number*

$$M_{ms} = \frac{V}{v_{ms}} > 1. \tag{2.5}$$

Collisionless shocks are often characterized by their *Alfvén Mach number*, defined as

$$M_A = \frac{V}{v_A}. \tag{2.6}$$

2.3 Rankine-Hugoniot relations

There are constraints that relate the unshocked upstream plasma to the shocked downstream plasma. These are called the Rankine-Hugoniot (RH) relations. We use the notation $[f] = f_u - f_d$, where the subscript u denotes upstream and d denotes downstream. Some plasma parameters like number density n, bulk velocity $\mathbf{V}$ and magnetic field $\mathbf{B}$ upstream and downstream of a shock is illustrated in Figure 2.2.

The first relation is mass conservation. The flux of mass in to the shock must be the same as out from it. In a frame where the shock is in rest, this can be expressed as

$$\hat{\mathbf{n}} \cdot [n\mathbf{V}] = 0, \tag{2.7}$$

where $\hat{\mathbf{n}}$ is the shock normal vector. Since the velocity is lower downstream of the shock, the density downstream of a shock is always greater than upstream. Additionally, the Maxwell equation $\nabla \cdot \mathbf{B} = 0$ leads to that the magnetic field going into the shock must be equal to the magnetic field going out of it, or

$$\hat{\mathbf{n}} \cdot [\mathbf{B}] = 0. \tag{2.8}$$

From Maxwell's equation $\nabla \times \mathbf{E} = -\partial \mathbf{B}/\partial t$ combined with the the ideal Ohm's law $\mathbf{E} + \mathbf{V} \times \mathbf{B} = 0$, we get

$$\hat{\mathbf{n}} \times [\mathbf{V} \times \mathbf{B}] = 0. \tag{2.9}$$

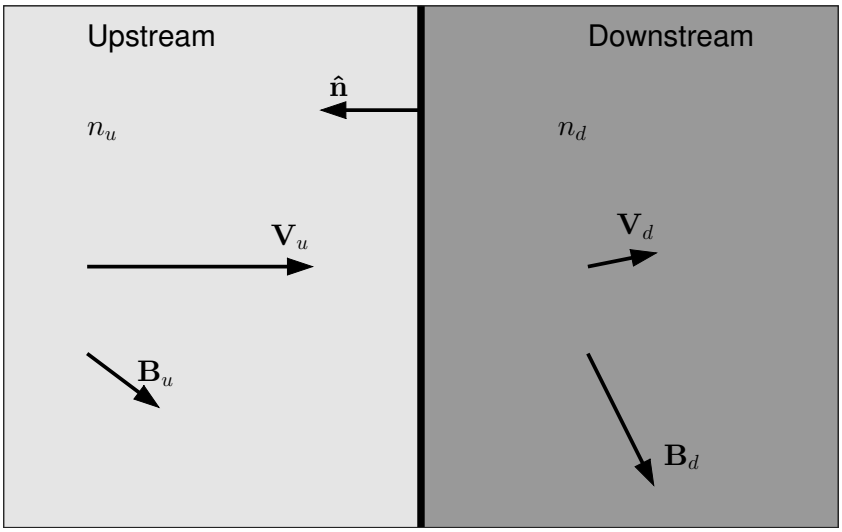

Figure 2.2. 2D illustration of the Rankine Hugoniot jump conditions. The shock is marked as a black line. Flow velocity and magnetic field are indicated by arrows, density is shown by shading.

Fast mode collisionless shocks always give rise to an increase in density, temperature and entropy when going from upstream to downstream. The density ratio describes the rate of compression of a shock and is defined as n_d/n_u. The density ratio increases with Mach number and in a single-species plasma, the maximum density ratio is 4. In this limit, the shock is referred to as a *strong shock*.

These relations and the remaining two relations related to momentum and energy conservation are derived from magnetohydrodynamic (MHD) equations, which employ a fluid description of the plasmas [Landau and Lifshitz, 1960]. MHD is a valid description on large scale. The shock itself is a very thin region and it excites turbulence, which makes the MHD equations break down at the shock. On these small scales, or kinetic scales, the particle dynamics become imoprtant and the fluid description is no longer valid. Therefore, the RH relations are only valid when measured sufficiently far up- and downstream of the shock. Figure 2.3 shows spacecraft measurements from one shock crossing. The data shows a long period of time in low time resolution and a shorter period with higher resolution data. At the large scales, the RH relations are mostly fulfilled while the situation is a lot more complicated at small scales. In spacecraft data, the RH relations are helpful when determining for example the speed and the normal vector of a shock.

2.4 Ion reflection

At shocks with $M_{ms} \sim 1-2$, V_d increases with increasing V_u. When a sufficiently high V_u, V_d is the same as the downstream magnetosonic speed. The

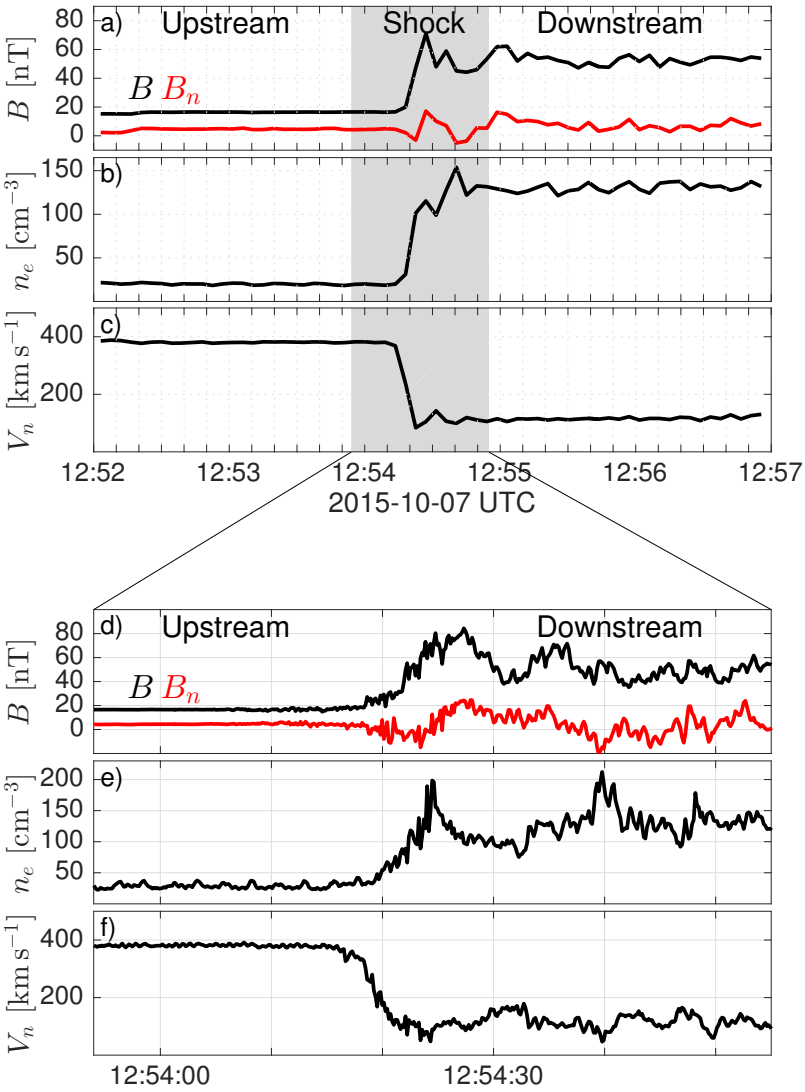

Figure 2.3. Plasma measurements of a shock crossing by one of the Magnetospheric Multiscale spacecraft. a)-c) A long period of time with 10 s resolution data, which corresponds to MHD scales. d)-f) zoomed-in view of the shock of data with 30 ms resolution, which corresponds to kinetic scales.

shock is then referred to as critical. The critical Mach number M_c depends on plasma β and θ_{Bn} and is $M_c \leq 2.76$. In the case of a supercritical shock where $M_{ms} > M_c$ the shock is no longer able to slow down the flow by dissipation alone. The influx of plasma into the shock is so great that energy dissipation is not fast enough to slow the plasma sub-magnetosonic speeds. The supercritical shock is then forced to reflect a portion of the incoming upstream ions, which lowers the inflow momentum and energy density.

We now consider a shock where the upstream magnetic field is along the shock surface or perpendicular to the shock normal, this is referred to as a perpendicular shock. This case is illustrated in Figure 2.4a. Here, an upstream ion is reflected off the shock surface. The reflection is usually considered specular, i.e. the normal component of the velocity changes sign but the tangential

velocity of the ion is conserved [Paschmann et al., 1980]. After the reflection, the ion gyrates around $\mathbf{B}_u$. However, the guiding center is convected towards the shock. This means that the ion is accelerated by the convection electric field $\mathbf{E}_u = -\mathbf{V}_u \times \mathbf{B}_u$. This is also illustrated in Figure 2.4b, that shows the same event in velocity space. The ion gyrates upstream of the shock with constant speed in the upstream frame. This is seen as a circle in velocity space with radius 2 $|\mathbf{V}_u \cdot \hat{\mathbf{n}}|$ centered around $\mathbf{V}_u$.

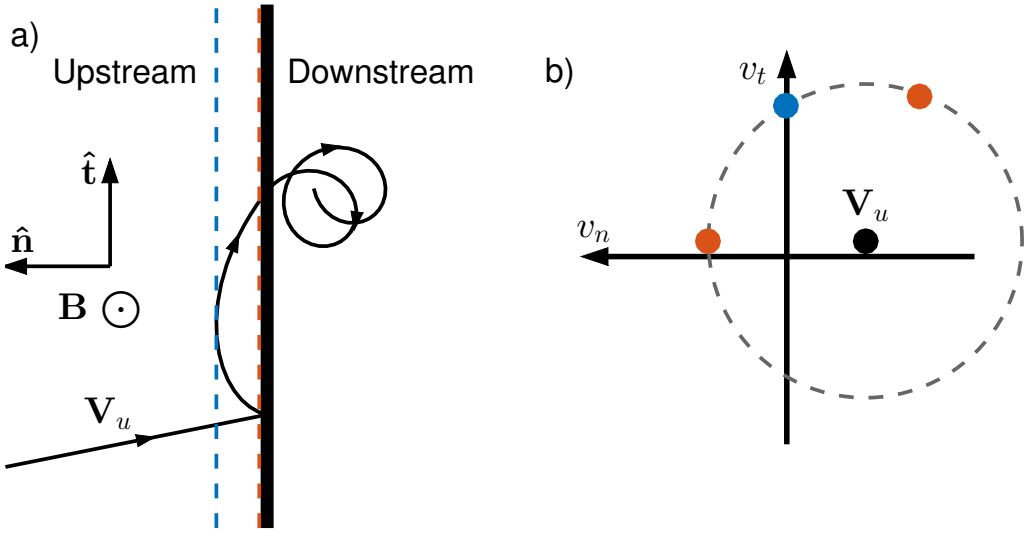

Figure 2.4. Illustration of ion reflection in real and velocity space. (a) Incoming ions with velocity $\mathbf{V}_u$ are specularly reflected off a shock. The ions return to the shock after one gyration around $\mathbf{B}_u$and penetrate downstream. (b) ion populations in velocity space. The dashed circle marks constant energy in the upstream frame. The velocities of reflected ions at two positions marked as dashed lines in (a) are shown: Red is just upstream of the shock, here there are both newly reflected ions and returning ions. Blue is the ion velocity at the turnaround distance, the ions are moving purely tangential to the shock.

When the ion returns to the shock the ion has a few times the energy of upstream ions. This allows the ion to penetrate the shock an pass downstream where it contributes to the heating of the plasma.

2.5 Shock geometry

Previously, we considered ions reflecting off a perpendicular shock. We now define an angle θ_{Bn} to be the acute angle between $\mathbf{B}_u$ and $\hat{\mathbf{n}}$. In the case of a perpendicular shock $\theta_{Bn} = 90°$, and for a parallel shock $\theta_{Bn} = 0°$. A shock with $\theta_{Bn} > 45°$ is referred to as *quasi-perpendicular* and a shock with $\theta_{Bn} < 45°$ as *quasi-parallel*.

In the subcritical regime, quasi-perpendicular and quasi-parallel shocks behave similarly. For supercritical quasi-perpendicular shocks, ions are reflected and reach the turnaround distance d before returning to shock. The region between the shock and the turnaround point forms the foot of the shock. In the case of supercritical quasi-parallel shocks, the reflected ions do not turn around but follow the magnetic field lines back upstream and therefore do not return to the shock. The reflected ions excite various instabilities. This creates an extended foreshock region with highly developed turbulence and upstream structures. The transition from upstream to downstream in quasi-parallel shocks is very extended and happens in several steps [Schwartz and Burgess, 1991].

3. The Earth system

3.1 The magnetosphere

The magnetosphere is the region of space that surrounds Earth. In the magnetosphere, the motion of charged particles is dictated by Earth's magnetic field. Due to the dynamic pressure of the solar wind, the magnetosphere is compressed on the day side and elongated on the night side, forming the magnetotail. Upstream of the magnetosphere, there is a bow shock that decelerates the solar wind, creating the magnetosheath. The boundary separating the magnetosphere and the magnetosheath is called the magnetopause. Figure 3.1 shows an illustration of the different regions of Earth's magnetosphere.

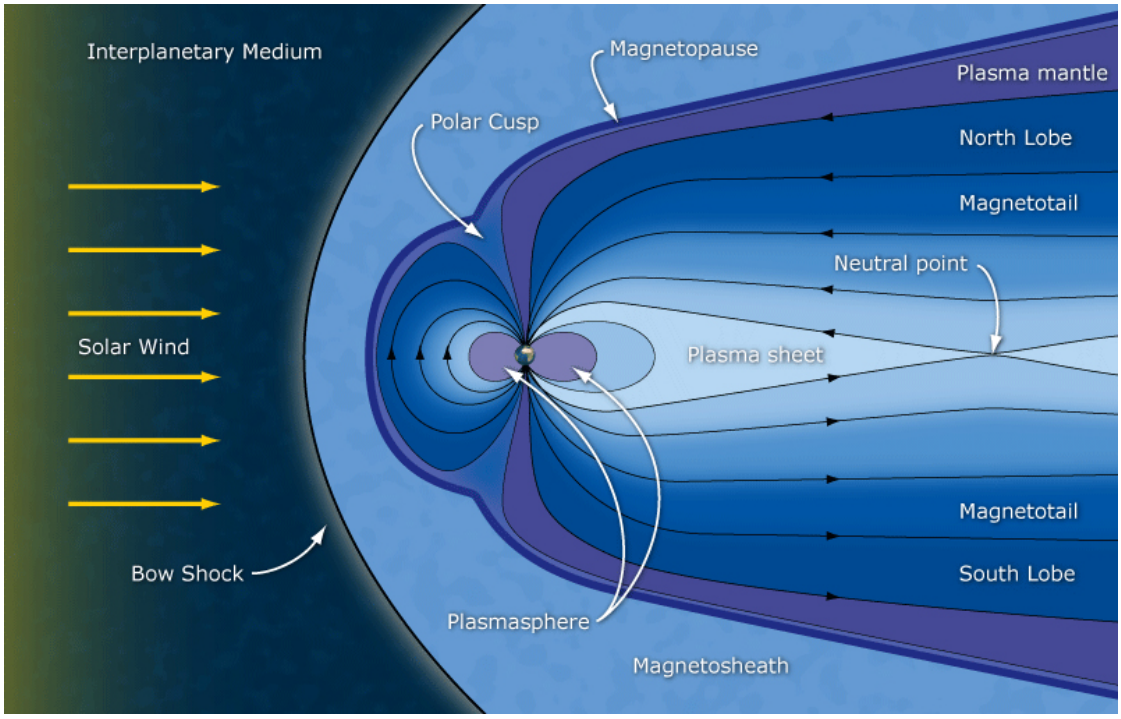

Figure 3.1. Illutration of Earth's magnetosphere. Image credit: ESA/C. T. Russell.

3.2 The bow shock

Earth's bow shock forms when the supersonic solar wind impacts the magnetosphere. Since the obstacle is blunt, the bow shock has a round shape, usually assumed to be a cylindrically symmetric conic section [Schwartz, 1998].

Under normal Parker spiral conditions [Parker, 1958], the interplanetary magnetic field at Earth is $\sim 45^\circ$ from the Earth-Sun line. This means that the dusk side of the bow shock is usually quasi-perpendicular while the dawn side is normally quasi-parallel. This is illustrated in Figure 3.2. This also shows the difference between the turbulent and extended quasi-parallel shock and the relatively sharp quasi-perpendicular shock.

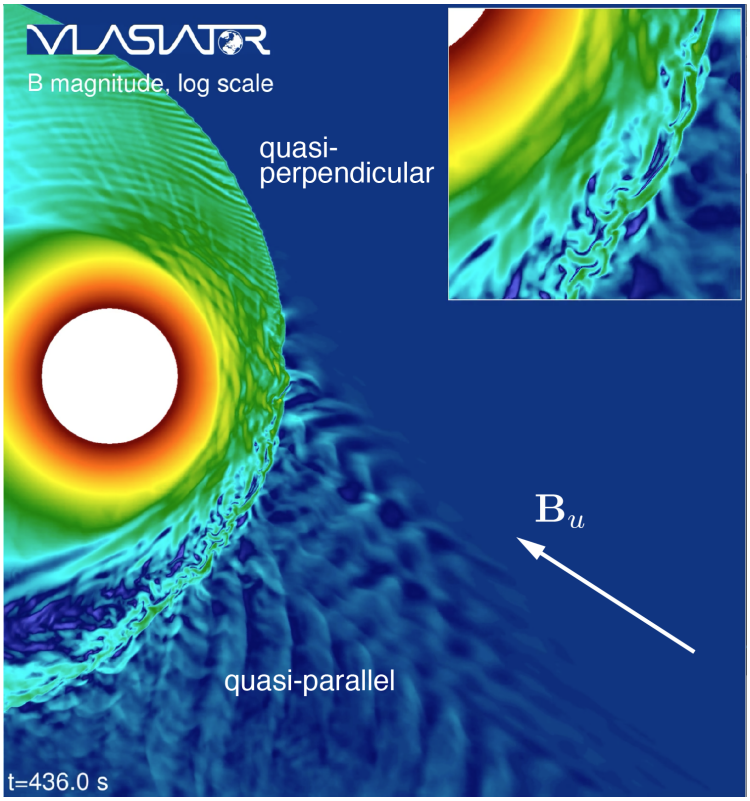

Figure 3.2. Global hybrid-Vlasov simulation of Earth's bow shock [von Alfthan et al., 2014], `http://vlasiator.fmi.fi/`. The solar wind arrives from the right in the figure. The quasi-parallel and quasi-perpendicular regions of the shock are indicated.

Earth's bow shock is in most cases a supercritical shock with $M_A \sim 10$. Figure 3.2 shows the Alfvén Mach number as a function of time over ~ 3 solar cycles. The density ratio of the bow shock is typically $2.5-4$ [Formisano et al., 1973].

Earth's bow shock is therefore a shock with variyng geometry and plasma parameters. Compared to for example SNR shocks, the bow shock is very small and has low Mach number compared to $M_A \sim 1000$ at SNRs [Reynolds, 2008]. Despite this, the bow shock is an excellent laboratory where models about shocks can be tested with in situ spacecraft measurents.

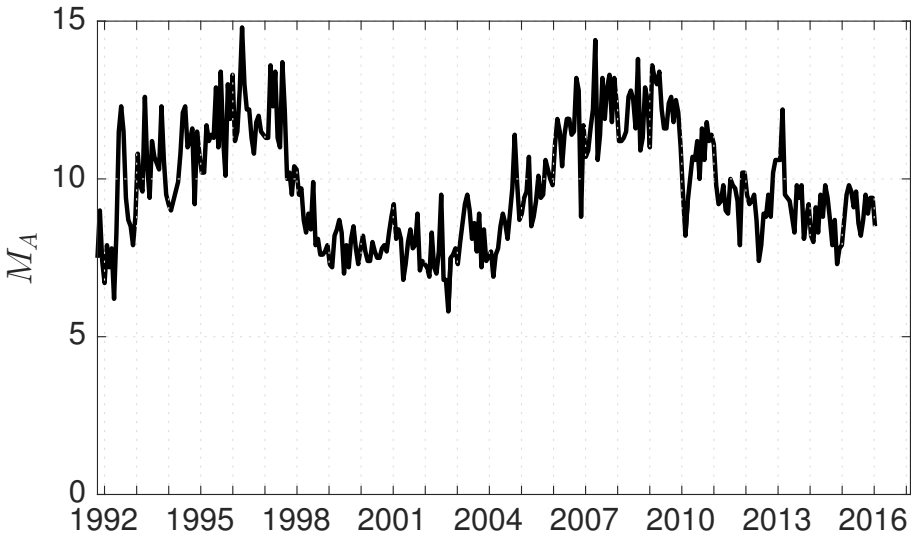

Figure 3.3. 27 day averages of Alfvén Mach number of the solar wind. There is a denpendence on the phase of the solar cycle and peaks during solar minimum. Data from the OMNI database: `http://omniweb.gsfc.nasa.gov`.

4. Spacecraft missions

4.1 Cluster

Cluster is an ESA mission to study Earth's plasma environment launched in 2000. The mission consists of four satellites flying in a tetrahedral formation with varying separation.

The satellites were launched into a highly elliptical polar orbit with an apogee of $\sim$19 Earth radii . With this orbit, Cluster can perform in situ studies in various regions like the solar wind, the bow shock, the magnetopause, the polar cusps and the magnetotail.

The Cluster spacecraft are cylindrical in shape and are rotating along the symmetry axis of the cylinder with a spin period of 4 seconds [Escoubet et al., 1997]. Cluster carries several instruments to measure various plasma parameters such as electric field, magnetic field and particle distributions of ions and electrons.

4.2 Magnetospheric MultiScale

The Magnetospheric MultiScale (MMS) mission is a NASA mission launched in 2014 and is studying small-scale processes in magnetic reconnection. Like Cluster, MMS consists of four identical spacecraft flying in a tetrahedron formation, although with a shorter spacecraft separation [Burch et al., 2016].

MMS is currently in an equatorial orbit with apogee $\sim 12 R_E$ which is designed to skim the magnetopause in order to encounter as many reconnection sites as possible. However, MMS has also encountered the solar wind and the bow shock several times at times when the magnetopause has been pushed closer to Earth.

Like Cluster, MMS has instruments to measure fields and particle distributions. The major advantage of MMS is that the particle distributions of ions and electrons are measured at much greater rate [Pollock et al., 2016]. This, together with the shorter spacecraft separation, means that MMS is able to resolve plasma physical processes at much smaller spatial and temporal scales.

5. Particle acceleration

5.1 Diffusive shock acceleration

In a paper, Fermi [1949] proposes a possible source for the origin of high energy cosmic rays. The mechanism works by particles being stochastically reflected off moving magnetic mirrors in the form of irregularities in the intergalactic magnetic field. A head-on collision with a mirror leads to an increase of the particle energy and when the particle catches up to mirror, the energy decreases. However, head-on collisions are more probable so, on average, the particle gains energy over time. On average, the energy gain per collision is

$$\left\langle \frac{\Delta E}{E} \right\rangle \propto \left(\frac{U}{c} \right)^2, \tag{5.1}$$

where U is the speed of the magnetic mirror. The power of 2 means this is a second order acceleration process. This leads to an exponential growth of the particle energy and a power-law energy distribution

$$N(E) \propto E^{-x}, \tag{5.2}$$

where $N(E)$ is the number density of particles with energy E. The fits the observations of cosmic rays, which show that the distribution has a power-law.

The modern view of cosmic ray acceleration involves strong shocks around SNRs and is called *diffusive shock acceleration* (DSA). The concept of DSA was conceived in the late 70's independently by [Axford et al., 1977], [Krymskii, 1977], [Bell, 1978], and [Blandford and Ostriker, 1978]. The mechanism is stochastic in nature and involves particles repeatedly crossing a shock front.

The process of DSA is illustrated in Figure 5.1, which shows a high energy particle crossing from the upstream to the downstream of a shock several times. On each side, the high energy particles are assumed to diffuse and form isotropic populations, while conserving energy in the local plasma frame. The diffusion happens by deflecting off structures and turbulence in the plasma. By this process the particles can be "reflected" back to the shock. In the shock frame, such reflections appear to change the energy of the the particles. As seen in Figure 5.1, a reflection from the upstream increases the energy and a reflection from the downstream decreases the energy.

On average for strong shocks, a particle gains energy each round trip. In the case where speed of the particle approaches c, the average energy gain is

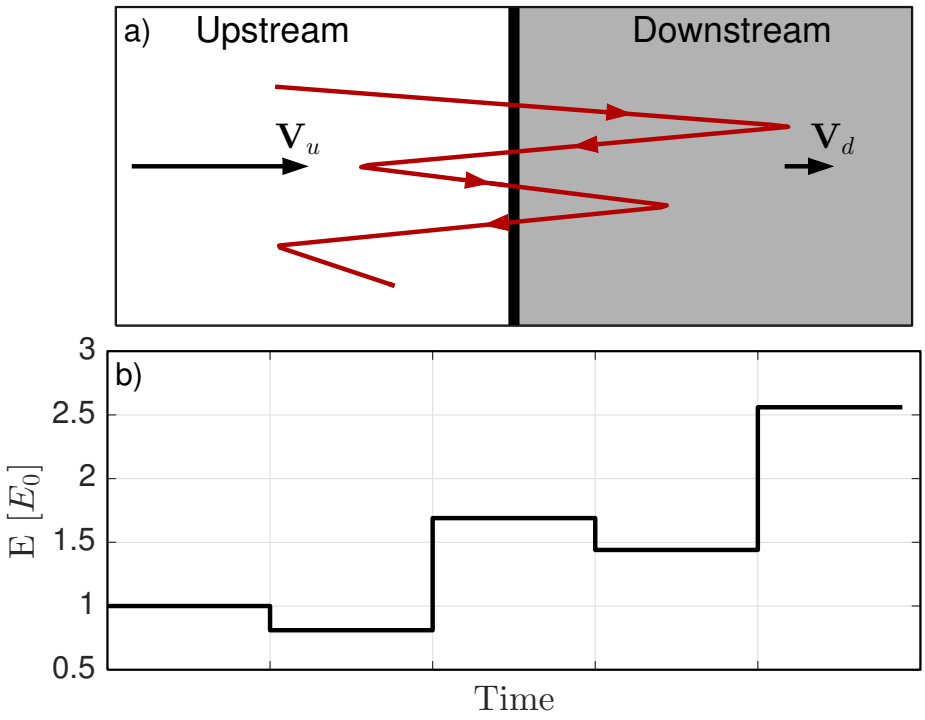

Figure 5.1. Illustration of DSA. a) trajectory of a high energy particle bouncing between upstream and downstream. b) energy of the particle as a function of time, where E_0 is the initial energy. On average, the energy increases.

$$\left\langle \frac{\Delta E}{E} \right\rangle \propto \frac{V_u}{c}, \tag{5.3}$$

which means DSA is a first order Fermi acceleration process. There is a certain probability $P \sim V_d/c$ that the particle will escape the system downstream. In the end the particle distribution becomes

$$N(E) \propto E^{-2}, \tag{5.4}$$

which is close to the observed power-law distribution of cosmic rays [Adriani et al., 2011].

The maximum energy essentially limited by the size of the system. In our galaxy, SNRs have very large and strong shocks and are potential acceleration sites for cosmic rays. Large fluxes of very high energy hadrons have been found in the vicinity of SNRs [e.g. Abdo et al., 2010, Morlino and Caprioli, 2012]. It has also been shown in observations and simulations that quasi-parallel shocks are more efficient for DSA than quasi-perpendicular shocks [e.g. Reynoso et al., 2013, Caprioli and Spitkovsky, 2014]. This is because quasi-parallel shock produce more turbulence up- and downstream on which the particles can be deflected.

5.2 The injection problem

The models of Fermi acceleration like DSA presuppose the existence of a population high energy particles, or suprathermal particles. The speed of the suprathermal particles must be much higher than the speed of the shock in order for them to cross the shock several times and not to be convected downstream. This means that particles from the thermal population must be preaccelerated before they can be injected into large scale DSA, and be accelerated to cosmic ray energies. Figure 5.2 shows distribution function illustrating the thermal and suprathermal populations.

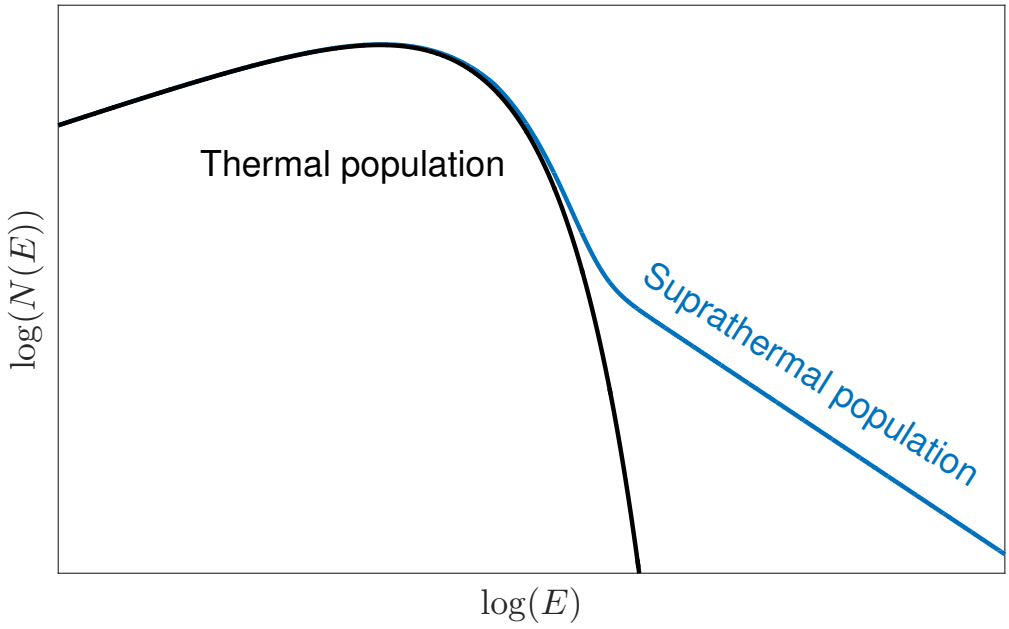

Figure 5.2. Illustration of thermal and suprathermal particle population. The thermal population in black has a Maxwellian distribution. The suprathermal population is seen as a high energy tail on the thermal population.

How particles can be injected problem is still an unsolved issue in shocks physics and in situ spacecraft observations are well suited to study these processes.

In a study using data from Cluster, Kis et al. [2013] found evidence of suprathermal ion injection at Earth's quasi-parallel bow shock. The proposed mechanism is gyrosurfing acceleration when a SLAMS merge with a wave packet, which has trapped ions [Kuramitsu and Krasnoselskikh, 2005].

Using 2D hybrid simulations, Caprioli et al. [2015] show ions being reflected off a quasi-parallel shock. The shock is self-reforming, which makes the reflection efficiency unsteady. The magnetic field upstream of the shock is magnified and turned so that the local shock geometry becomes quasi-perpendicular. This allows reflected ions to return to the shock and undergo several reflection, gaining energy each time.

In Paper I, we use Cluster data and show that ions can be accelerated in a process of being reflected off SLAMS and undergoing shock drift acceleration. This process is similar to [Caprioli et al., 2015] in that ions are reflected and accelerated. But instead of being reflected off a reforming shock surface the ions in our study are reflected off steepened upstream structures, or SLAMSs. Figure 5.2 shows this process.

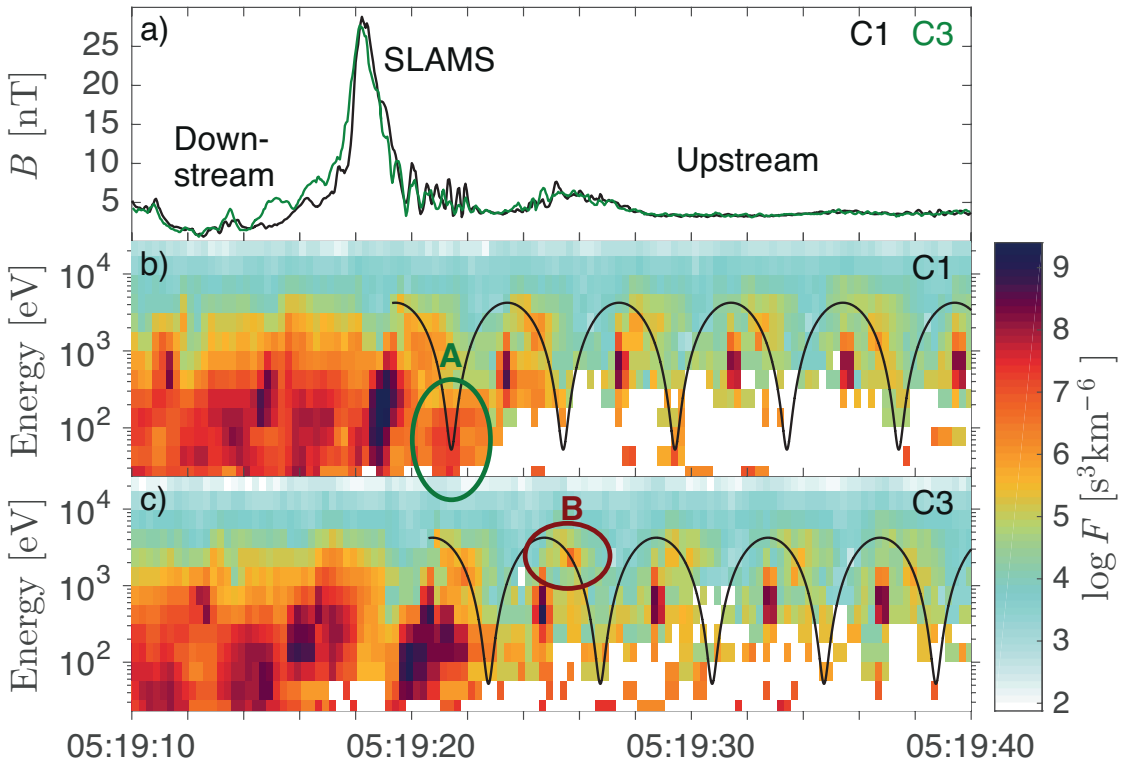

Figure 5.3. (a) Magnetic field magnitude. (b)–(c) Ion phase-space density averaged over polar angle in sub-spin resolution. Two ion populations upstream of the SLAMS are circled and denoted by A and B. A: Reflected ions just upstream of the SLAMS. B: Ions with higher energy than the solar wind; these ions are seen by both spacecraft and further upstream as well. The solid lines in panels (b) and (c) are theoretical curves for specular reflection. Figure 3 from [Johlander et al., 2016].

6. Shock non-stationarity

Under certain conditions a shock can become non-stationary. This means that even under stable upstream conditions, the structure and motion of the shock becomes unsteady and changes with time. Shock non-stationarity is linked to the ion dynamics at supercritical shocks and can take several forms. It was demonstrated in a laboratory plasma by Morse et al. [1972] after being theorized by Auer et al. [1962].

Shock-nonstationarity has been extensively studied in hybrid and fully kinetic numerical simulations. In a study using hybrid simulations by Leroy et al. [1982] showed that a shock can become unstable for $\beta \lesssim 0.6$ and $M_A \gtrsim 8$ due to over- and under reflection of ions. They reported that the magnetic field magnitude in the overshoot varies with 20% and the same variation in the amount of reflected ions. Simulations by [Lembege and Savoini, 1992] showed that a shock undergoes cyclic self-reformation, where a new shock is formed upstream of the existing shock and is then moves back downstream. The time of the reformation is equal to the ion gyrofrequency measured in the overshoot of the shock. In a study by Krasnoselskikh et al. [2002] the authors present a critical non-linear whistler Mach number,

$$M_{nw} = \sqrt{\frac{m_i}{2m_e}} \cos\theta_{Bn}, \tag{6.1}$$

above which non-linear whistler waves cannot exist in the shock ramp and the shock becomes non-stationary.

There have been few in situ spacecraft observations of shock non-stationarity. In a study using multi-spacecraft data from Cluster with a relatively large spacecraft separation, Lobzin et al. [2007] presented evidence for shock non-stationarity by observations of different magnetic structure of the shock for different spacecraft, as well as a time variability of reflected ions with a period of the order of the ion gyroperiod. In a study from Mercury, Sundberg et al. [2013] showed that observations of downstream fluctuations in the magnetosheath are consistent with a cyclic self-reformation of the shock front. Sulaiman et al. [2015] presented evidence of high Mach number shocks undergoing self-reformation at Saturn's bow shock using Cassini data.

An important kind of shock non-stationarity is rippling, which is a phenomenon where surface waves, or ripples, move along the shock surface. Hybrid 2D simulations of quasi-perpendicular shocks by Lowe and Burgess [2003] showed that ripples propagate along the magnetic field. Ripples have been shown to influence ion dynamics and acceleration processes of shocks

[e.g. Yang et al., 2012, Hao et al., 2016]. In simulations, ripples have been shown to accelerate electrons to high energies [Umeda et al., 2009]. In a study using Cluster data Moullard et al. [2006] exploits a slow and partial shock crossing to conclude that it is rippled.

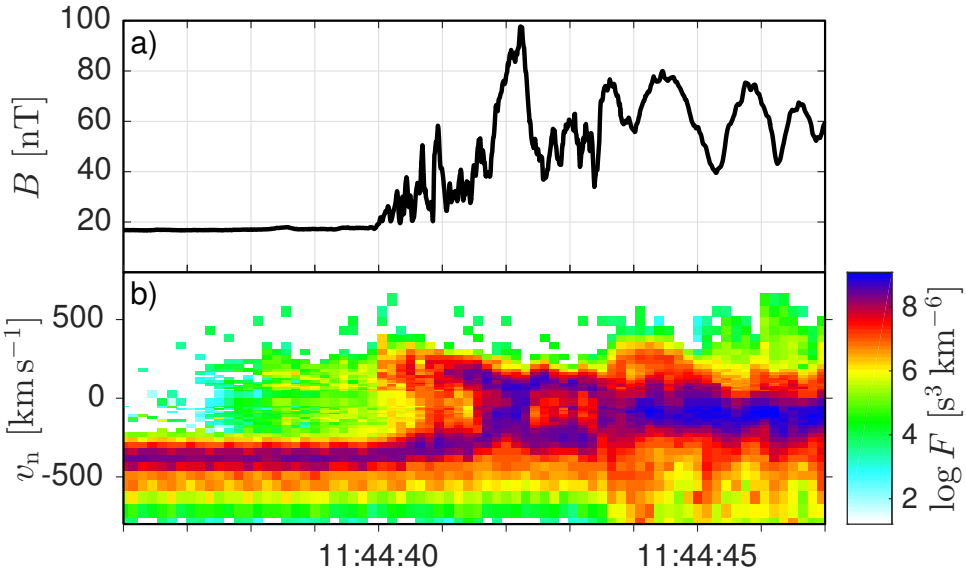

Figure 6.1. Example of MMS data used in Paper II. a) Magnetic field magnitude. b) Ion phase-space density as a function of normal speed. The spacecraft encounters the shock ramp and is later upstream of the ramp, seen by ion phase-space holes.

In Paper II, we use one rapid quasi-perpendicular shock crossing by MMS and find that it is rippled. We use the high cadence plasma measurements of MMS and find that the spacecraft encounter the shock and go back and fourth between up- and downstream, see Figure 6.1. We find this apparent motion of the shock to be consistent with ripples and that the characteristics of the ripples are in good agreement with simulations [Lowe and Burgess, 2003, Ofman and Gedalin, 2013]. Figure 6.2 shows a sketch of the event and shows the spacecraft trajectories through the rippled shock.

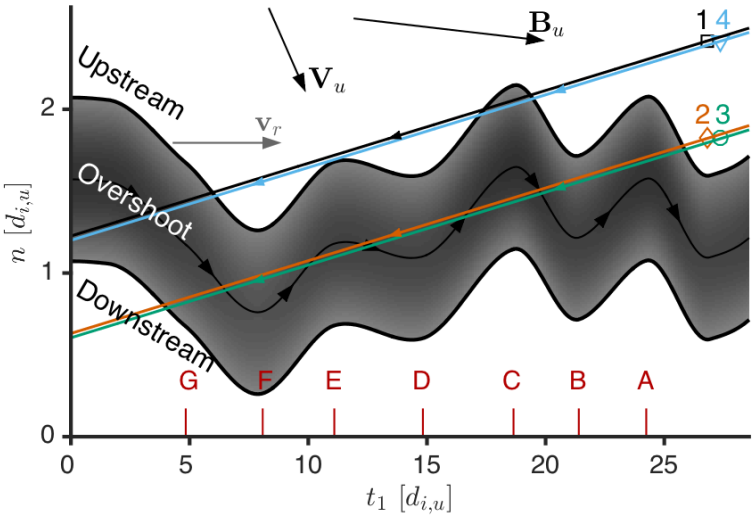

Figure 6.2. Spacecraft trajectories through the shock are illustrated by colored lines. Figure 5 in Paper II.

7. Outlook

Future work should include the role of upstream waves and 3D electric field in heating and acceleration of ions. There is also a prospect of investigating electron acceleration at rippled shocks. There is a wealth of MMS data from the shock. The high quality data of MMS provides a view of shocks in unprecedented detail.

8. Acknowledgments

I would like to thank my supervisors for their support and patience. I would also like to thank the Cluster instrument teams and the Cluster Science Archive as well as the MMS teams and the MMS Science Data Center for providing the data for these studies.

References

A. A. Abdo, M. Ackermann, M. Ajello, L. Baldini, J. Ballet, G. Barbiellini, M. G. Baring, D. Bastieri, B. M. Baughman, K. Bechtol, R. Bellazzini, B. Berenji, R. D. Blandford, E. D. Bloom, et al. Gamma-Ray Emission from the Shell of Supernova Remnant W44 Revealed by the Fermi LAT. *Science*, 327:1103, February 2010. doi: 10.1126/science.1182787.

O. Adriani, G. C. Barbarino, G. A. Bazilevskaya, R. Bellotti, M. Boezio, E. A. Bogomolov, L. Bonechi, M. Bongi, V. Bonvicini, S. Borisov, S. Bottai, A. Bruno, F. Cafagna, D. Campana, R. Carbone, P. Carlson, M. Casolino, G. Castellini, L. Consiglio, M. P. De Pascale, C. De Santis, N. De Simone, V. Di Felice, A. M. Galper, W. Gillard, L. Grishantseva, et al. PAMELA Measurements of Cosmic-Ray Proton and Helium Spectra. *Science*, 332:69, April 2011. doi: 10.1126/science.1199172.

P. L. Auer, H. Hurwitz, Jr., and R. W. Kilb. Large-Amplitude Magnetic Compression of a Collision-Free Plasma. II. Development of a Thermalized Plasma. *Physics of Fluids*, 5:298–316, March 1962. doi: 10.1063/1.1706615.

W. I. Axford, E. Leer, and G. Skadron. The acceleration of cosmic rays by shock waves. *International Cosmic Ray Conference*, 11:132–137, 1977.

A. R. Bell. The acceleration of cosmic rays in shock fronts. I. *Mon. Not. R. Astron. Soc.*, 182:147–156, January 1978. doi: 10.1093/mnras/182.2.147.

R. D. Blandford and J. P. Ostriker. Particle acceleration by astrophysical shocks. *Astrophys. J. Lett.*, 221:L29–L32, April 1978. doi: 10.1086/182658.

J. L. Burch, T. E. Moore, R. B. Torbert, and B. L. Giles. Magnetospheric Multiscale Overview and Science Objectives. *Space Sci. Rev.*, 199:5–21, March 2016. doi: 10.1007/s11214-015-0164-9.

D. Caprioli and A. Spitkovsky. Simulations of Ion Acceleration at Non-relativistic Shocks. I. Acceleration Efficiency. *Astrophys. J.,* , 783:91, March 2014. doi: 10.1088/0004-637X/783/2/91.

D. Caprioli, A.-R. Pop, and A. Spitkovsky. Simulations and Theory of Ion Injection at Non-relativistic Collisionless Shocks. *Astrophys. J. Lett.*, 798:L28, January 2015. doi: 10.1088/2041-8205/798/2/L28.

F. De Hoffmann and E. Teller. Magneto-hydrodynamic shocks. *Phys. Rev.*, 80: 692–703, Nov 1950. doi: 10.1103/PhysRev.80.692. URL `http://link.aps.org/doi/10.1103/PhysRev.80.692`.

C. P. Escoubet, C. T. Russell, and R. Schmidt. *The Cluster and PHOENIX missions*. 1997.

E. Fermi. On the Origin of the Cosmic Radiation. *Physical Review*, 75:1169–1174, April 1949. doi: 10.1103/PhysRev.75.1169.

V. Formisano, P. C. Hedgecock, G. Moreno, F. Palmiotto, and J. K. Chao. Solar wind interaction with the Earth's magnetic field: 2. Magnetohydrodynamic bow shock. *J. Geophys. Res.*, 78:3731, 1973. doi: 10.1029/JA078i019p03731.

Y. Hao, Q. Lu, X. Gao, and S. Wang. Ion Dynamics at a Rippled Quasi-parallel Shock: 2D Hybrid Simulations. *Astrophys. J.*, 823:7, May 2016. doi: 10.3847/0004-637X/823/1/7.

A. Johlander, A. Vaivads, Y. V. Khotyaintsev, A. Retinò, and I. Dandouras. Ion injection at Quasi-parallel Shocks Seen by the Cluster Spacecraft. *Astrophys. J. Lett.*, 817:L4, January 2016. doi: 10.3847/2041-8205/817/1/L4.

A. Kis, O. Agapitov, V. Krasnoselskikh, Y. V. Khotyaintsev, I. Dandouras, I. Lemperger, and V. Wesztergom. Gyrosurfing Acceleration of Ions in Front of Earth's Quasi-parallel Bow Shock. *Astrophys. J. Lett.*, 771:4, July 2013. doi: 10.1088/0004-637X/771/1/4.

V. V. Krasnoselskikh, B. Lembège, P. Savoini, and V. V. Lobzin. Nonstationarity of strong collisionless quasiperpendicular shocks: Theory and full particle numerical simulations. *Physics of Plasmas*, 9:1192–1209, April 2002. doi: 10.1063/1.1457465.

G. F. Krymskii. A regular mechanism for the acceleration of charged particles on the front of a shock wave. *Akademiia Nauk SSSR Doklady*, 234:1306–1308, June 1977.

Y. Kuramitsu and V. Krasnoselskikh. Gyroresonant Surfing Acceleration. *Physical Review Letters*, 94(3):031102, January 2005. doi: 10.1103/PhysRevLett.94.031102.

L. D. Landau and E. M. Lifshitz. *Electrodynamics of continuous media*. 1960.

B. Lembege and P. Savoini. Nonstationarity of a two-dimensional quasiperpendicular supercritical collisionless shock by self-reformation. *Physics of Fluids B*, 4: 3533–3548, November 1992. doi: 10.1063/1.860361.

M. M. Leroy, D. Winske, C. C. Goodrich, C. S. Wu, and K. Papadopoulos. The structure of perpendicular bow shocks. *J. Geophys. Res.*, 87:5081–5094, July 1982. doi: 10.1029/JA087iA07p05081.

V. V. Lobzin, V. V. Krasnoselskikh, J.-M. Bosqued, J.-L. Pinçon, S. J. Schwartz, and M. Dunlop. Nonstationarity and reformation of high-Mach-number quasiperpendicular shocks: Cluster observations. *Geophys. Res. Lett.*, 34:L05107, March 2007. doi: 10.1029/2006GL029095.

R. E. Lowe and D. Burgess. The properties and causes of rippling in quasi-perpendicular collisionless shock fronts. *Annales Geophysicae*, 21:671–679, March 2003. doi: 10.5194/angeo-21-671-2003.

G. Morlino and D. Caprioli. Strong evidence for hadron acceleration in Tycho's supernova remnant. *Astron. Astrophys.*, 538:A81, February 2012. doi: 10.1051/0004-6361/201117855.

D. L. Morse, W. W. Destler, and P. L. Auer. Nonstationary Behavior of Collisionless Shocks. *Phys. Rev. Lett.*, 28:13–16, January 1972. doi: 10.1103/PhysRevLett.28.13.

O. Moullard, D. Burgess, T. S. Horbury, and E. A. Lucek. Ripples observed on the surface of the Earth's quasi-perpendicular bow shock. *J. Geophys. Res. (Space Physics)*, 111:A09113, September 2006. doi: 10.1029/2005JA011594.

L. Ofman and M. Gedalin. Rippled quasi-perpendicular collisionless shocks: Local and global normals. *J. Geophys. Res. (Space Physics)*, 118:5999–6006, October 2013. doi: 10.1002/2013JA018780.

E. N. Parker. Dynamics of the Interplanetary Gas and Magnetic Fields. *Astrophys. J.*, 128:664, November 1958. doi: 10.1086/146579.

G. Paschmann, N. Sckopke, J. R. Asbridge, S. J. Bame, and J. T. Gosling. Energization of solar wind ions by reflection from the earth's bow shock. *J. Geophys. Res.*, 85:4689–4693, September 1980. doi: 10.1029/JA085iA09p04689.

C. Pollock, T. Moore, A. Jacques, J. Burch, U. Gliese, Y. Saito, T. Omoto, L. Avanov, A. Barrie, V. Coffey, et al. Fast Plasma Investigation for Magnetospheric Multiscale. *Space Sci. Rev.*, 199:331–406, March 2016. doi: 10.1007/s11214-016-0245-4.

S. P. Reynolds. Supernova Remnants at High Energy. *Annu. Rev. Astron. Astrophys.*, 46:89–126, September 2008. doi: 10.1146/annurev.astro.46.060407.145237.

E. M. Reynoso, J. P. Hughes, and D. A. Moffett. On the Radio Polarization Signature of Efficient and Inefficient Particle Acceleration in Supernova Remnant SN 1006. *Astron. J.*, 145:104, April 2013. doi: 10.1088/0004-6256/145/4/104.

S. J. Schwartz. Shock and Discontinuity Normals, Mach Numbers, and Related Parameters. *ISSI Scientific Reports Series*, 1:249–270, 1998.

S. J. Schwartz and D. Burgess. Quasi-parallel shocks - A patchwork of three-dimensional structures. *Geophys. Res. Lett.*, 18:373–376, March 1991. doi: 10.1029/91GL00138.

A. H. Sulaiman, A. Masters, M. K. Dougherty, D. Burgess, M. Fujimoto, and G. B. Hospodarsky. Quasiperpendicular High Mach Number Shocks. *Phys. Rev. Lett.*, 115(12):125001, September 2015. doi: 10.1103/PhysRevLett.115.125001.

T. Sundberg, S. A. Boardsen, J. A. Slavin, V. M. Uritsky, B. J. Anderson, H. Korth, D. J. Gershman, J. M. Raines, T. H. Zurbuchen, and S. C. Solomon. Cyclic reformation of a quasi-parallel bow shock at Mercury: MESSENGER observations. *J. Geophys. Res. (Space Physics)*, 118:6457–6464, October 2013. doi: 10.1002/jgra.50602.

T. Umeda, M. Yamao, and R. Yamazaki. Electron Acceleration at a Low Mach Number Perpendicular Collisionless Shock. *Astrophys. J.*, 695:574–579, April 2009. doi: 10.1088/0004-637X/695/1/574.

S. von Alfthan, D. Pokhotelov, Y. Kempf, S. Hoilijoki, I. Honkonen, A. Sandroos, and M. Palmroth. Vlasiator: First global hybrid-Vlasov simulations of Earth's foreshock and magnetosheath. *Journal of Atmospheric and Solar-Terrestrial Physics*, 120:24–35, December 2014. doi: 10.1016/j.jastp.2014.08.012.

Z. W. Yang, B. Lembège, and Q. M. Lu. Impact of the rippling of a perpendicular shock front on ion dynamics. *J. Geophys. Res. (Space Physics)*, 117:A07222, July 2012. doi: 10.1029/2011JA017211.